Desalination and Water Treatment
www.deswater.com

34 (2011) 123–128
October

1944-3994/1944-3986 © 2011 Desalination Publications. All rights reserved
doi: 10/5004/dwt.2011.2853

Electro-microfiltration of the mineral particles in dairy processing

Frank G.F. Qin[a,*], John Mawson[b], Xin An Zeng[c]

[a]*Research Center of Distributed Energy Systems, DongGuan University of Technology, Dong Guan City, China*
Tel. +86-0769-22862619; Fax: +86-0769-22861808; email: qingf@dgut.edu.cn
[b]*Institute of Food, Nutrition & Human Health, Massey University, New Zealand*
[c]*South China University of Technology, Guangzhou, China*

Received 3 September 2010; Accepted 3 January 2011

ABSTRACT

Two sintered stainless steel (SSS) microfiltration membranes (5 μm and 25 μm pore size respectively) were used for separating Alamin particles found in dairy processing. An external electric field was applied upon the membrane to provide a combination of rejective coulomb force, fluid shearing force and the bubbling rejection to the foulant. The electric field can be applied in two ways: 1) to mitigate the fouling deposit, and/or 2) to clean the fouled filtering surface. The divergence of pH in the retentate and permeate was studied.

Keywords: Electro-microfiltration; Membrane; Separation; Sintered stainless steel

1. Introduction

Since most fine particulate substances (colloids) acquire a surface electric charge when in contact with a polar medium (e.g., water), resulting in an electric double layer (EDL) [1] in the vicinity around the particle surface. Electro-filtration makes use of an electric field to increase the rate of filtration by providing an additional electrostatic rejection force to the particles to mitigate fouling [2–8]. When the field is applied to microfiltration (MF), the process is called electromicrofiltration (EMF). This has raised interest in the field of membrane separation, especially in bioseparation in recent years [9–12].

Sintered Stainless Steel (SSS) membrane has unique advantage in strength and chemical inertness, it can withstand harsh chemical and physical cleaning as well as high pressure back-flushing [13–15]. It is also electro conductive, thus an electric field can be applied upon the membrane module. By taking the advantage of electric rejection, electrofiltration has great potential to enhance the existing filtration processes (e.g., by increasing the throughput in existing plants or by reducing production cost), to develop new fractionated products based on differences in molecular charge, or to remove foulant.

2. Apparatus and materials

The experimental apparatus of this study comprised a cross-flow microfiltration membrane module, a 30 l feed tank, a 0.75 kw gear pump, a tubular heat-exchanger (which maintained a constant solution temperature), 5 valves, a pair of pressure transducers (P_{in} and P_{out}, 0~4 bar), which measured the trans-membrane pressure (TMP) and a XTRAVERT® AC motor speed controller (mode X302, PDL Electronic LTD, Napier, NZ) to adjust the pump speed. A typical arrangement of the system is shown in Fig. 1.

Two SSS membranes were used in this work. They were supplied by Industrial Research Limited (NZ). The module construction, as shown in Fig. 2, makes it highly resistant to organic and inorganic solvents, and can be used at high pressure (15~40 bar) and high temperature (>200°C) [16]. The difference between the membranes was their mean pore size: 5 μm nominal pore size of the smaller one and 25 μm for the other. The tubular membrane and the central bar (also stainless steel) composed a pair of electrodes when they were electrically charged.

*Corresponding author.

Presented at the AMS6/IMSTEC10, The 6th conference of the Aseanian Membrane Society in conjunction with the 7th International Membrane Science and Technology Conference, Sydney Australia, November 22–26, 2010

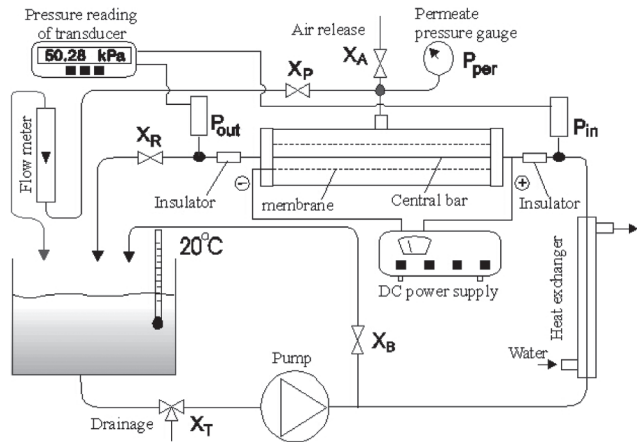

Fig. 1. Schematic diagram of the system arrangement.

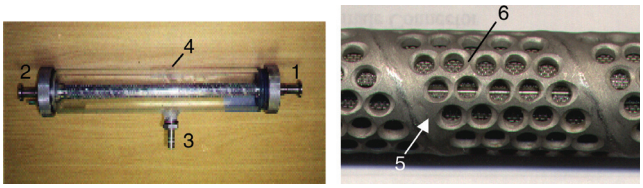

Fig. 2. The SSS membrane module. 1) feed inlet. 2) retentate outlet. 3) permeate outlet. 4) Perspex jacket. 5) backing hull of the tubular membrane. 6) SSS membrane.

The perspex jacket collected the permeate and returned it back to the feed tank. Key dimensions of the membrane are shown in Table 1.

As the membrane was electrically charged, water was electrolysed with the formation of gas bubbles. The impacts of electrochemical reactions on the membrane and solution cannot be ignored. Thus the electric current density on the membrane also needed to be carefully controlled. This was done by pre-setting the output current and voltage of the DC power supply (0~50 V, 0~3 A). A pair of plastic fittings was used at the inlet and outlet of the module as the electric insulator.

Table 1
Dimensions of two membrane modules

Membrane tube inner diameter	φ13.5 mm
Effective length	380 mm
Central bar diameter	φ8 mm
Nominal pore size	5 μm for the small pore size membrane and 25 μm for the large pore size membrane
Filtration area	0.019 m^2

Two kinds of fine particles, Alamin and calcite, were used in this study. The former was a by-product of the dairy industry separated from whey. It is a complex substance mainly composed of calcium phosphate. The latter was prepared by chemical deposition. Their particle morphologies are similar. The major focus was on the behaviour of the Alamin suspension, and the calcite was used as comparison.

3. Experimental method

The suspensions were prepared and stored in a cylindrical tank, and pumped to feed the tubular membrane module as shown in Fig. 1. The concentration of particles (Alamin or calcite) was 0.07%~1%(w/v). The retentate recycled back to the tank. A by-pass stream was maintained with valve X_B to achieve dual functions: to agitate the suspension in the tank and to adjust the feed pressure (coupling with the adjustment of pump speed and the opening of the valve, X_R). The pressure of the feed stream (P_{in}) and retentate stream (P_{out}) were measured with an inlet and an outlet transducer. The permeate pressure (P_{per}) was measured with a pressure gauge. A flowmeter was used to measure the permeate flow before it returned to the tank.

The membrane can be positively or negatively charged. However, since the fine particles in most of the actual colloidal system generally appear as negative zeta potential in a neutral pH range, thus a negatively charged membrane is repulsive to the deposit particles. Moreover, the cathode current on the membrane provide an electrochemical protection to the membrane from being electrochemically corroded as well. A heat exchanger was employed to maintain a constant temperature of 20°C, and a gas-release channel (via valve V_A) was used to minimize the gas-bubble disturbance to the flowmeter readings.

4. Results and discussions

4.1. Membrane polarity and properties

The electrode current varying with the applied voltage is shown in Fig. 3, where the SSS membrane worked as an anode in curve 1, but as a cathode in curve 2, 3 and 4. The calcite concentration for curve 1 and 2 was 0.7% (wt), for curve 3 was 0.07% (wt), for curve 4 was zero.

Experiments showed that i) the electrode current was approximately proportional to the voltage applied and the particle content in the suspension; ii) when the membrane was negatively charged and worked as a cathode, the membrane current was twice as large as the case when it was positively charged at the same voltage.

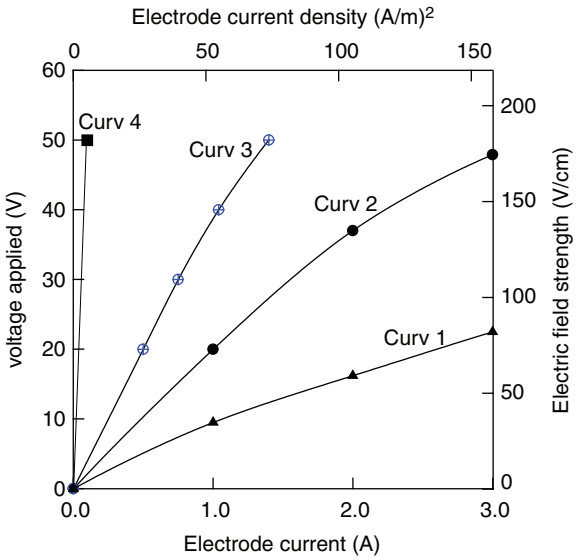

Fig. 3. Dependence of the electrode current on the voltage applied.

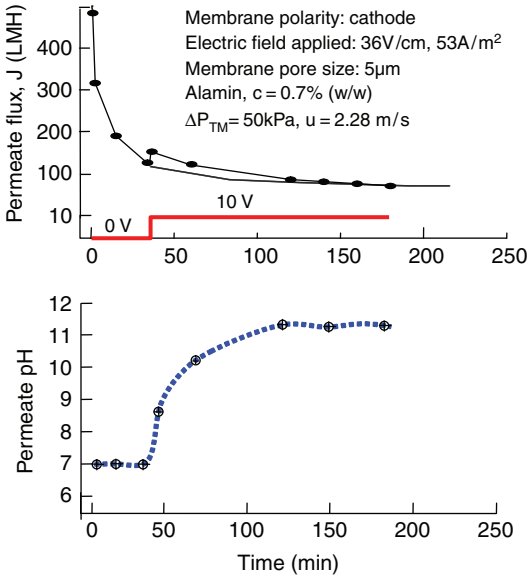

Fig. 4. Influence of the electric field to the flux decline.

Since the membrane surface area was twice the central bar of the module, implying that the electrolytic current was proportional to the cathode area. This can be explained by the fact that the hydrogen ion, a proton (H^+), was the fastest electrophoretic ion amongst all the ions and, it was the only ion undergone the electrode reduction on the cathode in this system. Thus a larger cathode area would allow more protons to be converted to hydrogen gas in a unit time resulting in a higher electrode current.

4.1.1. EMF with a negatively charged membrane

The application of EMF for separating Alamin particles with a negatively charged membrane is shown in Fig. 4, in which an electric field was applied at the 40th min after the filtration started. The observed permeate flux increased almost immediately when the field was applied. Nevertheless, the permeate flux declined gradually after reaching the maximum. Its pH was measured as well, which increased from 7 to 11. The initial flux gain (ΔJ) was about 25 $l \cdot m^{-2} \cdot h^{-1}$. The dashed line under the peak represents the possible trend of the permeate flux if the membrane was not charged. Further study revealed that the rapid increase of permeate reading was attributed to the generation of hydrogen gas on the cathode membrane, as such, the permeate alkalization was due to protons (H^+) consumption on the cathodic membrane.

A manually controlled pulsatile application of EMF with negatively charged membrane is shown in Fig. 5. The voltage was 50 V(DC), i.e., at about 180 $V \cdot cm^{-1}$ electric field strength, and the electric charge time was 2 min.

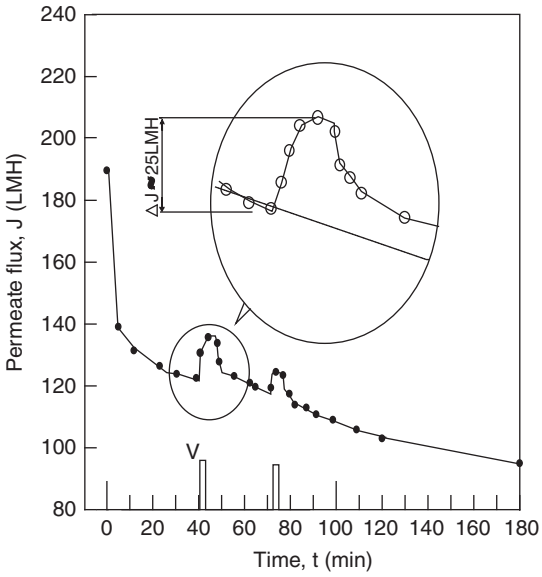

Fig. 5. The EMF flux gain of alamin (ΔJ) when electric field was been applied. Membrane pore size: 5 μm, pH=7, ΔP_{TM}=6.5 kPa, u=0.7 m/s, Field strength: 180 V/cm, Current I=63 A/m^2.

The membrane current was 1.2 A, giving a current density of 63 $A \cdot m^{-2}$.

It was observed that the gas bubbles that were formed on the cathode and carried by the permeate disturbed the flowmeter's reading and gave a false higher apparent permeate flux right after the power was switched on. The reason for emphasizing the bubble effect is that this seems not to be mentioned and taken into consideration by some earlier researchers [2,7,8,17].

To distinguish the bubble influence from the true permeate flux, a measuring cylinder and stopwatch were used to measure the flow rate and the result was then compared with the result of the flowmeter, these are shown in Fig. 6. The permeate flux gain measured with the flowmeter was about 50% higher than that measured with cylinder and stopwatch. Note that the gas-releasing channel was closed in this run to force the gas bubbles to pass through the flowmeter.

The permeate flux gain (ΔJ), shown in Fig. 6, was measured at the steady state: a low transmembrane pressure (3.5 kPa) was maintained stably under which the permeate flux was lower than the critical flux and no obvious flux decline was observed for a long time [18,19]. After the electric field was applied, the permeate flux gradually increased and reached a maximum value in about 5~10 min. The higher the voltage, the greater the electric current, and the larger the flux gain. After the flux reached to the maximum, it gradually decreased again no matter whether the electric field maintained or not, thus the variation of the flux produced a peak. The flux difference between the peak and the original level is defined as the permeate flux gain, as shown in Fig. 6.

As the permeate was found alkalizing when the SSS membrane worked as a cathode, a further experiment was carried out to trace the pH change of the permeate, retentate and bulk suspension in the storage tank, during which the permeate and retentate were both returned to the storage tank and mixed. Samples were collected every 10 min and measured with a pH meter. The result is shown in Fig. 7. The permeate pH increased as usual but the retentate pH decreased in the first 20 min, and then increased as well. The whole suspension in the storage tank was pH 7.7–7.8 at the end of the experiment, slightly increased from the original pH 7.2.

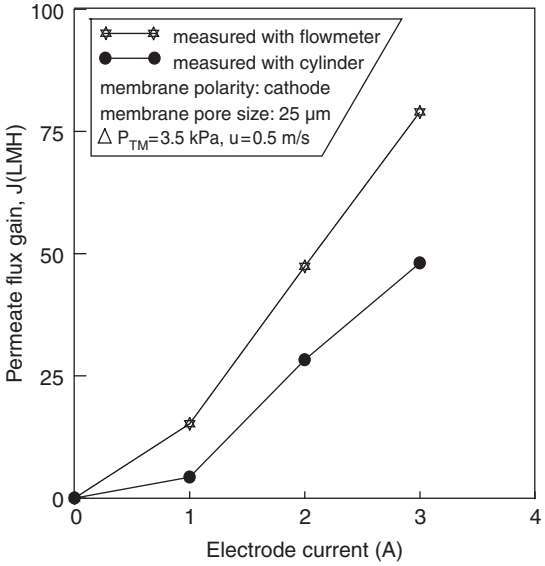

Fig. 6. The permeate flux gain ΔJ varies with cathode current strength.

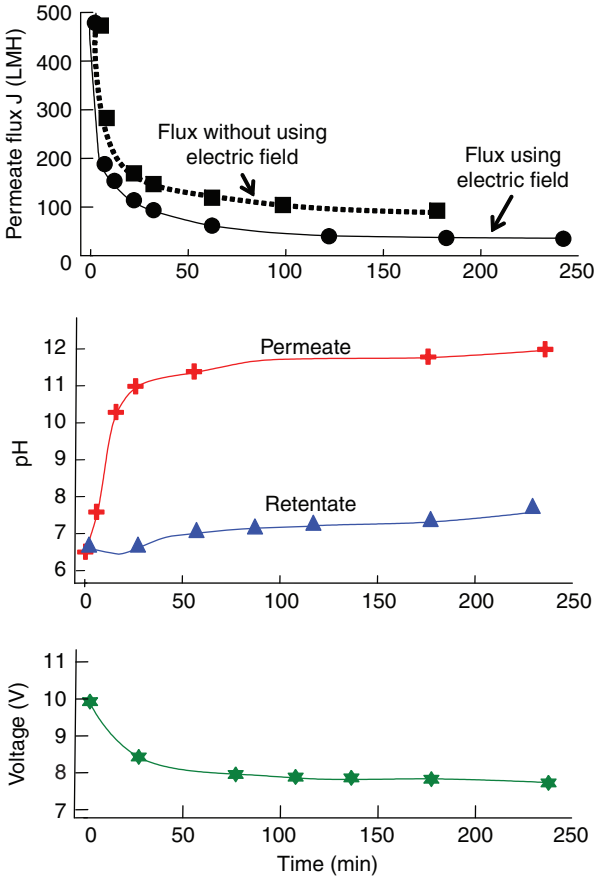

Fig. 7. The pH divergence of the permeate and retentate in a continuous run of EMF, in which the membrane worked as a cathode (Electric field applied: 53 A·m^{-2}. Alamin particle c = 0.7%(w/v), ΔP_{TM}=50 kPa, u=2.28 m·s^{-1}).

4.1.2. EMF with a positively charged membrane

The results of EMF experiments using a positively charged membrane are shown in Fig. 8. In contrast to the negatively charged operation, the permeate pH reached a lower point (e.g., pH≈3.5), and the permeate flux at 150 mins was 65% higher than that of the uncharged membrane and was about 300% higher than the negatively charged membrane. The generation of hydrogen ions (H^+) on the anode (membrane) was the reason for permeate acidification. This in turn resulted in the dissolving of calcium salt foulant and reduced membrane fouling. Despite the electrical attraction of the negatively charged particles by the membrane, the overall effect was that the permeate flux increased compared to the experiment without using an electric field.

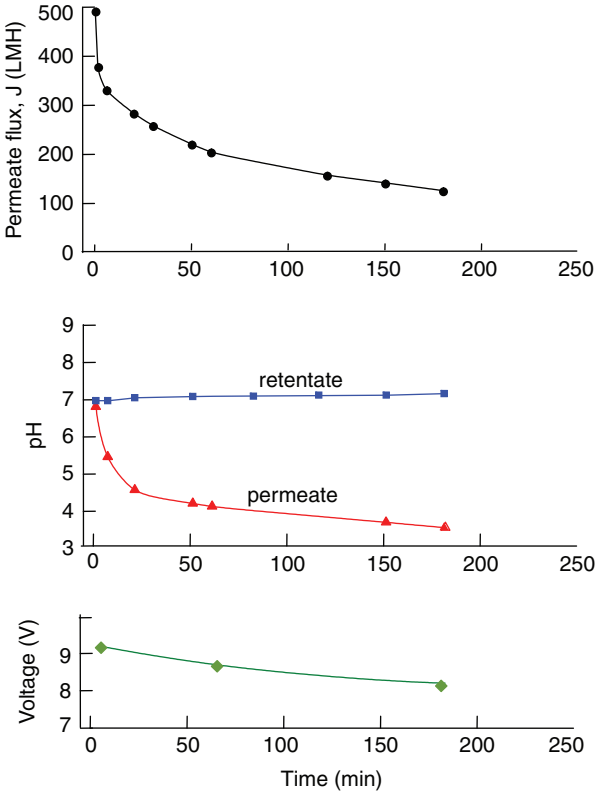

Fig. 8. Continuous EMF with positively charged membrane. Membrane polarity: anode. Constant electrode current density: 53Am^{-2}. Membrane pore size: 5 μm. Alamin content: 0.7 %(w/v), ΔP_{TM}=50 kPa, u=2.28 m·s^{-1}.

However, when the SSS membrane was positively charged, it was subject to the risk of anodic etching. Though the suspensions used in this study were all prepared with deionized water, we still found the electro conductivity of the suspension was much greater than the deionized water itself, indicating that the Alamin and calcite particles used in this study contained a little amount of soluble salts as impurities. The electro oxidation-reduction of acid radicals (e.g., Cl^{-1} at equation (4)) on the anodic membrane might cause corrosion. So the number of trials and the time using the membrane as an anode were all limited in this study to avoid damaging the membrane.

During the EMF, when the Alamin suspension was alkalized by the cathode reaction, newly-formed tiny particles of calcium salt would appear in the solution. Since the solubility of calcium salt is very low compared to the solid content of the suspension (e.g., the solubility of calcium carbonate is 1.53 × 10^{-3} g/ per 100 g H_2O at room temperature [20], but the solid content in the suspension for this study was ~0.7 g per 100 g H_2O), these newborn particles will not alter the total solid content of the suspension obviously. However, the newborn particles (new phase) would have a higher surface energy, this makes them easier to be adsorbed on the membrane surface. Moreover, it is on the membrane surface that the suspension is subject to greatest pH change (alkalised). The newborn particles are mainly form close to the cathodic membrane, this will induce more fouling of Alamin.

4.1.3. Electro cleaning in back flushing

The sintered stainless steel membrane is particularly suitable to restore its filterability by using the back flushing because of its mechanical strength. The gas bubbles formed underneath the foulant is effective in removing the foulant layer on the membrane surface outside the pore canal. However it is less effective for cleaning the inside pore fouling.

This explains the experimental results shown in Fig. 9, where the filterability, expressed in water flux (LMH). In the first group of experiments, the water flux was restored only 66% by back-flushing the 25 μm membrane (Fig. 9C). To restore more than 90% of the filterability, acid wash must be used (Fig. 9E). The external electric field showed improving the cleaning when it was applied during the back flush, but the water flux was not satisfactorily restored (Fig. 9D).

As for the cleaning of the 5 μm membrane shown by the second group of experiments in Fig. 9F~J, back flush restored 75% filterability, and achieved 85% if the external electric field was applied, indicating the electric field was working more effective for the small pore size membrane. On the other hand, since the particle size was 5 μm in this study, the above results can further be interpreted as there was more inside pore fouling in the 25 μm membrane than that in the 5 μm membrane; the electric field cleaned the external fouling better.

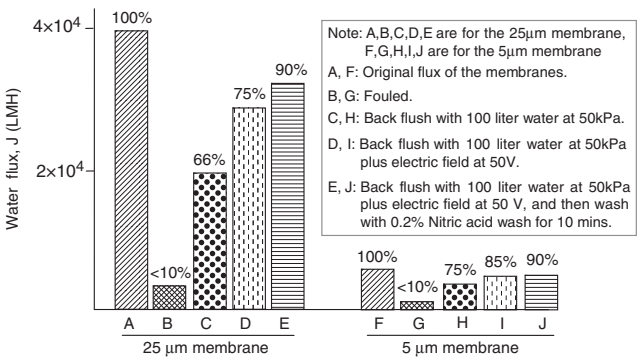

Fig. 9. Cleaning and restoring of the membranes.

5. Conclusion

The application of electro-microfiltration for separating Alamin and/or calcite particles from the suspensions resulted in an improvement in the permeate flux after a 180 Vcm^{-1} field strength of the static electric field was applied, in which the membrane was recommended working as a cathode to avoid being electro etched. The imposed static electric field was found functioning in the following ways:

1. The Alamin and calcite particles were subject to rejective coulomb force from the membranes, which was opposite the driving force of the filtration.
2. Electrolysis diverged the pH of the permeate and retentate. The permeate became alkaline but the retentate became acidic when the membrane worked as a cathode. If the ionic strength in dispersing solution is high, Electrochemical corrosion can not be ignored.
3. Newly formed tiny gas bubbles on the membrane surface underneath the foulant layer produced a dislodging effect that helped to detach the fouling. This effect was found particularly useful when (fresh) water was used for back flushing.
4. When the pulsatile electric field is used for electrofiltration, a DC power supply with an adjustable pulse output is recommended. The amplitude and period of the pulses should be determined in accordance with the change of the physical-chemical properties of the suspensions. The typical parameter used in this study is 0–50 V pulse height, 0–5 min pulse width and 0.05 $A \cdot cm^{-2}$ current density.

Special caution should be taken to avoid electrochemical corrosion when the stainless steel membrane works as an anode. Low ionic strength in the dispersing solution and a mild electric field should be used.

Acknowledgement

This research was sponsored by the 973 Program (2010CB227306) and NSFC(50836005) of China.

References

[1] M.F.C. Ladd, *Introduction to physical chemistry*, 1986, New York: Cambridge University Press.
[2] R.J. Wakemam, Eletriofiltration: Microfiltration plus eletrophoresis, The Chemical Engineer, 1986(June): 65–70.
[3] J.M. Radovich and B. Behnam, Steady-state modelling of electroultrafiltration at constant concentrations, Sep. Sci. Technol., 20(4) (1985) 315–329.
[4] P. Moulik, Physical aspects of electrofiltration, Environ. Sci. Technol., 5(9) (1971) 771–776.
[5] J.D.J. Henry, L.F. Lawler and C.H.A. Kuo, A solid/liquid separation process process based on cross flow and electrofiltration, American Institute of Chemical Engineers Journal, 23(6) (1977) 851.
[6] G. Akay and R.J. Wakemam, Electric field intensification of surfactant mediated separation, Chem. Eng. Res. Des., 74(5) (1996) 517–525.
[7] R.J. Wakemam and M.N. Sabri, Utilising Pulsed Flow Electriic Field in Crossflow Microfiltration of Titania Suspension, Transaction of the Institute of Chemical Engineers, 1995(a) 455–463.
[8] R.J. Wakemam and E.S. Tarleton, Experiments using electricity to prevent Fouling in Membrane Filtration, Filtration and Separation, 1986(May/June) 174–176.
[9] W.R. Bowen, A.N. Filippov, A.O. Sharif, V.M. Starov, A model of the interaction between a charged particle and a pore in a charged membrane surface, Adv. Colloid Interface Sci., 81(1) (1999) 35–72.
[10] W.R. Bowen, N. Hilal, M. Jain, R.W. Lovitt, A.O. Sharif and C.J. Wright, The effects of electrostatic interactions on the rejection of colloids by membrane pores---visualisation and quantification, Chem. Eng. Sci., 54(3) (1998) 369–375.
[11] Xiao Dong Chen, Dolly X.Y. Li, Sean X.Q. Lin and, Ozkan, N., On-line fouling/cleaning detection by measuring electric resistance--equipment development and application to milk fouling detection and hemical cleaning monitoring, J. Food Eng., 2003.
[12] W.R. Bowen and X. Cao, Electrokinetic effects in membrane pores and the determination of zeta-potential, J. Membr. Sci., 140(2) (1998) 267–273.
[13] M.S.A. Heikkinen and N.H. Harley, Experimental invetigation of sintered porous metal filters, J. Aerosol Sci., 31(6) (2000) 721–738.
[14] MSS., Micro-steel Caustic Recovery System, Mem-Brine System, in Membane System Specialists, 1995: Wisconsin Rapids, WI.
[15] Separations, G., Lit. No.s-106, Glasgow, DE. 1996.
[16] P. Neumann, Sintered metal filters benifit from asymmetric design, Filtration & Separation, 2000, July/August: 26–28.
[17] C.J. Reeve, Characterisation of an electromicrofiltration unit for use in bio-separation processes, in Institute of Food, Nutrition and Human Health, 1997, Massey University, New Zealand: Auckland (Albany campus).
[18] R.W. Field, D. Wu, J.A. and B.B.G. Howell, Critical flux concept for microfiltration fouling, J. Membr. Sci., 100 (1995) 259–272.
[19] J.A. Howell, Sub-critical flux operation of mecrofiltration, J. Membr. Sci., 107 (1995) 165–171.
[20] David R. Lide (Editor-in-chief) CRC Handbook of Chemistry and Physics. 76th ed., 1995–1996: 6–159.